7202 *Biochemistry* **2010,** *49,* 7202–7209
DOI: 10.1021/bi100147w

BIOCHEMISTRY
including biophysical chemistry & molecular biology
Article

Changes in Small-Angle X-ray Scattering Parameters Observed upon Binding of Ligand to Rabbit Muscle Pyruvate Kinase Are Not Correlated with Allosteric Transitions†

Aron W. Fenton,*,‡ Rachel Williams,‡ and Jill Trewhella§,||

‡*Department of Biochemistry and Molecular Biology, The University of Kansas Medical Center, MS 3030, 3901 Rainbow Boulevard, Kansas City, Kansas 66160,* §*School of Molecular and Microbial Biosciences, The University of Sydney, Sydney, NSW 2006, Australia, and* ||*Department of Chemistry, The University of Utah, 315 South 1400 East, Room 2020, Salt Lake City, Utah 84112-0850*

Received January 29, 2010; Revised Manuscript Received July 16, 2010

ABSTRACT: Protein fluorescence and small-angle X-ray scattering (SAXS) have been used to monitor effector affinity and conformational changes previously associated with allosteric regulation in rabbit muscle pyruvate kinase (M_1-PYK). In the absence of substrate [phosphoenolpyruvate (PEP)], SAXS-monitored conformational changes in M_1-PYK elicited by the binding of phenylalanine (an allosteric inhibitor that reduces the affinity of M_1-PYK for PEP) are similar to those observed upon binding of alanine or 2-aminobutyric acid. Under our assay conditions, these small amino acids bind to the protein but elicit a minimal change in the affinity of the protein for PEP. Therefore, if changes in scattering signatures represent cleft closure via domain rotation as previously interpreted, we can conclude that these motions are not sufficient to elicit allosteric inhibition. Additionally, although PEP has similar affinities for the free enzyme and the M_1-PYK−small amino acid complexes (i.e., the small amino acids have minimal allosteric effects), PEP binding elicits different changes in the SAXS signature of the free enzyme versus the M_1-PYK−small amino acid complexes.

The pyruvate kinase isozyme found in brain and muscle (M_1-PYK)[1] is inhibited by phenylalanine. This inhibition results in a decreased affinity of the enzyme for its substrate, phosphoenolpyruvate (PEP) (*1*, *2*). Although the physiological relevance of this regulation is not fully understood, this system has become a model for the study of heterotropic allostery [i.e., the impact that binding of one ligand to a protein has on the affinity of the protein for a second, chemically nonidentical ligand (*3*)]. High-resolution structures determined by X-ray crystallography demonstrate that each subunit of the homotetramer contains a single active site and a single amino acid binding site (*4*). Each subunit contains three domains; the active site lies between the two most N-terminal domains (i.e., A and B domains). In an attempt to gain insight into how the allosteric and active sites communicate, a previous study using neutron scattering identified a contraction or expansion of M_1-PYK upon binding of substrate or effector (*5*). These results were interpreted as indicating a cleft closure resulting from the rotation of the B domain with respect to the rest of the monomer (i.e., cleft closure of the active site). Similarly, comparisons of protein structures of multiple PYK isozymes with and without various ligands bound have been used to support a mechanism by which rigid domains rotate with respect to each other in the allosteric mechanism of PYK isozymes (*6*−*8*).

In a previous study, we demonstrated that for the interaction between M_1-PYK and amino acid effectors, the L-2-aminopropanaldehyde moiety of the amino acid ligand is most important for binding to the enzyme (*4*). The length of the hydrophobic side chain is responsible for determining the magnitude of the amino acid-dependent shift in the affinity of the protein for PEP. Small amino acids like alanine and serine can bind to the allosteric site on the protein but are unable to modify the affinity of the protein for PEP. In this work, the phenylalanine versus small amino acid comparison has been used in combination with fluorescence intensity and small-angle X-ray scattering (SAXS) measurements to further investigate what role the amino acid-elicited conformational changes might play in the allosteric mechanism.

MATERIALS AND METHODS

Materials. M_1-PYK purified from rabbit muscle was purchased from Roche Applied Science. Phenylalanine and the potassium salt of PEP were purchased from Fluka. Alanine and serine were purchased from Fisher Scientific. 2-Aminobutyric acid was produced by Aldrich. Other buffer components were from Fisher Scientific or Sigma.

Ligand-Induced Changes in Protein Fluorescence. The apparent affinity of M_1-PYK for PEP was determined by monitoring the intrinsic protein fluorescence while varying the PEP concentration. The intensity of M_1-PYK fluorescence, at 2 mg/mL, was measured in a 0.4 cm^2 cuvette using a PTI steady-state fluorometer equilibrated at 11 °C. Excitation was at 300 nm, and emission was collected as the area under the peak from 310 to 460 nm. Titration experiments were performed in 50 mM Tris-HCl (pH 9.0), 10 mM $MgCl_2$, and 0.1 mM EDTA with a range of concentrations

†This work was supported by National Institutes of Health Grant DK78076 (to A.W.F.) and Australian Research Council Federation Fellowship FF0457488 (to J.T.). The scattering experiments were performed at The University of Utah, supported by U.S. Department of Energy Grant DE-FG02-05ER64026 (to J.T.).

*To whom correspondence should be addressed: Department of Biochemistry and Molecular Biology, The University of Kansas Medical Center, MS 3030, 3901 Rainbow Blvd., Kansas City, KS 66160. Phone: (913) 588-7033. Fax: (913) 588-9896. E-mail: afenton@kumc.edu.

[1]Abbreviations: PYK, pyruvate kinase; M_1-PYK, pyruvate kinase isozyme found in mammal brain and muscle; PEP, phosphoenolpyruvate; E, free enzyme complex; EA, substrate−enzyme complex; EX, enzyme−effector complex.

 Published on Web 07/16/2010

of the respective amino acid as designated. Stock solutions of amino acids and PEP were adjusted to pH 9.0 before addition. KCl was added so that the final K^+ concentration in the cuvette was 500 mM before the addition of titrant [originally 500 mM K^+ was used both to maintain some level of consistency with previous experiments (*4*) and to minimize the percent change in K^+ due to additions with ligands; however, attempts to reduce the K^+ or ionic strength caused the protein to show signs of aggregation in SAXS studies]. Via addition of the respective amino acid concentration to all PEP additions, the amino acid concentration was kept constant over the PEP titration. Total PEP was corrected for bound PEP to derive free PEP. Blank readings of buffer alone were subtracted from measured values.

Data were fit to appropriate equations using the nonlinear least-squares fitting analysis of Kaleidagraph (Synergy). The apparent affinity of M_1-PYK for PEP ($K_{app\text{-}PEP}$) was obtained by fitting the fluorescence intensity (F) as a function of PEP concentration to

$$F = \frac{\Delta F[\mathrm{PEP}]^n + F_0(K_{app\text{-}PEP})^n + F_0[\mathrm{PEP}]^n}{K_{app\text{-}PEP}{}^n + [\mathrm{PEP}]^n} \quad (1)$$

where F is the intensity, F_0 is the intensity in the absence of effector, ΔF is the maximum change in intensity, $K_{app\text{-}PEP}$ is the concentration of PEP that yields a change in intensity equal to one-half ΔF, and n is the Hill coefficient. Midpoint values are termed $K_{app\text{-}PEP}$, rather than $K_{d\text{-}PEP}$, because changes in fluorescence intensity are not always directly proportional to ligand−protein complex formation with this enzyme (*9*). For the same reason, only qualitative conclusions are drawn from $K_{app\text{-}PEP}$ data. $K_{app\text{-}PEP}$ values were plotted as a function of amino acid concentration to display general trends in the data. When these data are presented on a log−log graph (e.g., Figure 2), the allosteric coupling between PEP and the effector is the difference between the two data plateaus at low and high concentrations of amino acids (*10*−*13*).

SAXS Data Acquisition and Analysis. Samples for SAXS measurement were prepared in 50 mM Tris-HCl (pH 9.0, 11 °C), 10 mM $MgCl_2$, and 0.1 mM EDTA. When present, the desired amino acid at 100 mM or K-PEP at 2.0 mM was included; indications of saturating conditions for each ligand are from Figure 2 and our previous study (*4*). As in fluorescence studies, KCl was added such that the total K^+ concentration in the solution was 500 mM. After the M_1-PYK was dialyzed into the desired condition, protein concentration values as determined by absorbance [absorbance at 280 nm of a 1 mg/mL solution at 1 cm = 0.54 (*14*)] were 12−20 mg/mL. The dialysates were used for measurement of solvent blanks to be subtracted from the scattering from each protein sample to obtain the SAXS signal due to the proteins. Data acquisition times for all samples and solvent blanks were 1 h, with the temperature maintained at 11 °C.

SAXS data were collected using the small-angle instrument at The University of Utah (described in ref *15*) and were reduced to $I(q)$ versus q and analyzed as previously described (*15*). $I(q)$ is the scattered X-ray intensity per unit solid angle, and q is the amplitude of the scattering vector, given by $4\pi(\sin\theta)/\lambda$, where 2θ is the scattering angle and λ is the wavelength of the scattered X-rays (1.54 Å).

Scattering data were initially subjected to Guinier analysis to check for the expected linearity of the Guinier plots for monodisperse samples, and then $P(r)$ analyses were performed using GNOM (*16*) with corrections for the slit geometry of the scattering instrument. $P(r)$ is the frequency of vector lengths connecting small-volume elements within the entire volume of the scattering particle, weighted by their scattering contrast. For a uniform scattering density object, $P(r)$ goes to zero at the maximum dimension, d_{max}, of the object. The radii of gyration (R_g) were calculated as the second moment of $P(r)$. Analysis of the forward scattering, $I(0)$, values normalized by protein concentration, in milligrams per milliliter, volume, and mean contrast was used to check that the scattering particles were monodisperse. As an additional check on the monodispersity of the samples, estimates for the volume of the scattering particles were obtained using the Porod invariant (*17*) and compared to expected particle volumes. All errors quoted are based on propagated counting statistics.

RESULTS

Allostery As Monitored by Ligand-Induced Changes in Protein Fluorescence. Comparative studies reported here were motivated by our previous findings that monitored the (initial velocity derived) apparent affinity of M_1-PYK for PEP over a concentration range of various amino acids (*4*). The most relevant results from that study can be summarized as follows. (1) Phenylalanine allosterically decreases the affinity of M_1-PYK for its substrate, PEP. (2) Small amino acids like alanine and serine bind competitively with phenylalanine but elicit negligible change in the affinity of the protein for PEP. (3) 2-Aminobutyric acid binds competitively with phenylalanine and elicits a small allosteric response.

The previous study was conducted at 30 °C and, because of the use of initial velocity measurements, in the presence of the second substrate, MgADP. To stabilize the protein during data collection, SAXS measurements reported here were taken at 11 °C in the absence of ADP. As a means of verifying the previous conclusions under the same conditions used to collect SAXS data, ligand-induced changes in protein fluorescence intensity were used to monitor ligand binding. When binding to free M_1-PYK, amino acids caused an increase in fluorescence intensity that was dependent on the type of amino acid (Figure 1). This increase followed the previous trend in the data of the ability of the amino acids to influence PEP affinity (*4*), with phenylalanine eliciting the largest increase in fluorescence intensity (32%), followed by 2-aminobutyric acid (24%) and alanine (19%). Serine did not appreciably alter fluorescence intensity. Binding of PEP to free M_1-PYK caused little, if any, change in fluorescence intensity. PEP titrated into M_1-PYK with an amino acid previously bound caused a decrease in intensity proportional to the increase in intensity that resulted from the addition of the amino acid. Regardless of the order of addition, the ternary complex is generated. The fluorescence intensity of this ternary complex with both the amino acid and PEP bound to M_1-PYK is very similar to that of the free M_1-PYK protein alone.

Changes in protein fluorescence intensity caused by PEP titrations were used to evaluate PEP affinity over a range of amino acid concentrations (Figure 2). As previously observed (*4*), phenylalanine reduces the affinity of M_1-PYK for PEP, but alanine causes a minimal change in the $K_{app\text{-}PEP}$. Under our conditions, the response of $K_{app\text{-}PEP}$ to 2-aminobutyric acid is not different from the response to alanine, a result that differs from the previous observations (*4*). The Hill numbers associated with PEP binding increased from 1 to 2.3 as the phenylalanine concentration increased but remained constant (= 1) over the concentration range of either alanine or 2-aminobutyric acid. As serine (and therefore PEP titrated in the presence of serine) does not elicit a change in protein fluorescence intensity, the response

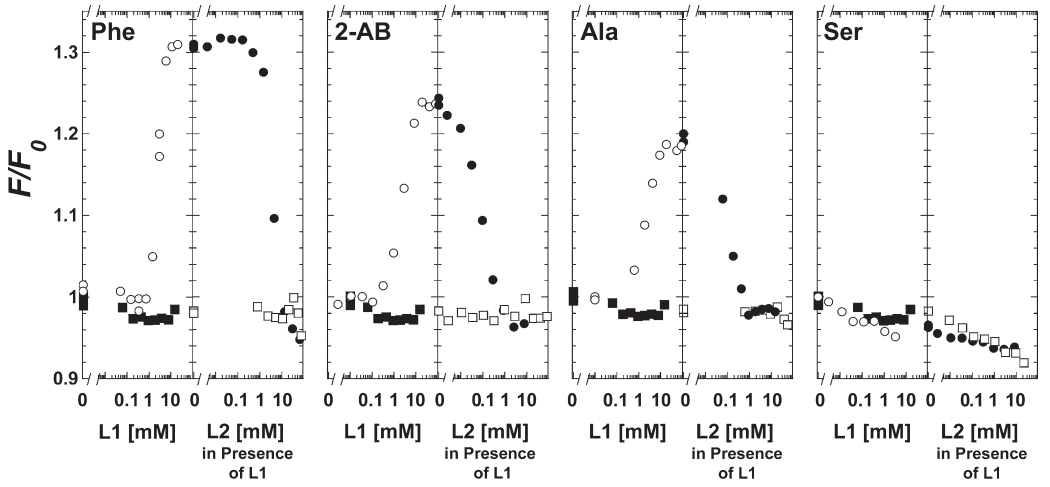

FIGURE 1: Changes in the steady-state intrinsic fluorescence intensity of M_1-PYK induced by amino acids and PEP. Panels are labeled by amino acid type (2-AB is 2-aminobutyric acid). In the left portion of each panel, free M_1-PYK was titrated with ligand 1 (L1), where L1 was either an amino acid (○) or PEP (■). In the right portion of each panel, M_1-PYK previously saturated with L1 was titrated with ligand 2 (L2). When L2 was an amino acid and M_1-PYK was presaturated with 10 mM PEP, data are represented as □. When L2 was PEP and M_1-PYK was presaturated with amino acid, data are represented as ●, Concentrations of amino acids used in these titrations were as follows: 96 mM phenylalanine [solubility limited, not completely saturating in the presence of PEP (see Figure 2)], 25 mM 2-aminobutyric acid, 30 mM alanine, and 40 mM serine.

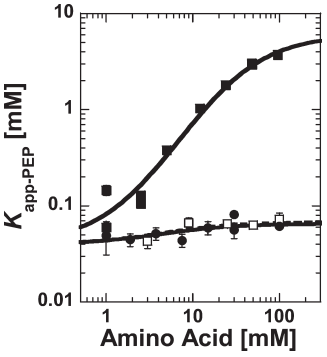

FIGURE 2: $K_{app\text{-}PEP}$ values determined by ligand-induced changes in protein fluorescence plotted as a function of the concentration of phenylalanine (■), alanine (●), or 2-aminobutyric acid (□). Here, the magnitude of the allosteric coupling is the distance between the top and bottom plateaus. The minimal fluorescence change caused by PEP binding in the absence of amino acids limits the ability to determine $K_{app\text{-}PEP}$ at amino acid concentrations of < 1 mM. Lines represent trends in the data.

of $K_{app\text{-}PEP}$ to this amino acid was not determined. Note that because of the solubility limits of phenylalanine, even the highest obtainable concentrations of phenylalanine were not completely saturating in the presence of PEP (i.e., at the highest phenylalanine concentration used in Figure 2, the top plateau is not fully formed).

SAXS Profiles of Enzyme Complexes. The measured $I(q)$ profile and corresponding $P(r)$ profile [calculated as the inverse Fourier transform of $I(q)$] for M_1-PYK with and without phenylalanine are shown in Figure 3, and the basic structural parameters derived for the protein in each ligand-bound state (as well as other enzyme complexes discussed below) are listed in Table 1. $P(r)$ is simply the probable distribution of distances between scattering centers within the scattering particle and goes to zero at the maximum linear dimension, d_{max}. Of note, the variations in the determined d_{max} values are insignificant (all in the range of 108−112 Å with estimated uncertainties of 2−3 Å, based on the fact that d_{max} values in this range showed no statistically significant difference in the quality of fit to the scattering data as estimated by χ^2 values). The R_g values show only small variations, and there are subtle yet statistically significant variations in the distribution of the frequency of vector lengths in the $P(r)$ functions. These latter variations are most easily seen in the difference $P(r)$ functions [$\Delta P(r)$] that reveal shifts in the distribution of the frequency of vector lengths that are characteristic of a small redistribution of mass within the tetramer that would result from domain or subunit rotations. The small scale of these ligand-induced changes is similar to those observed with neutron scattering, i.e., those previously interpreted as "cleft closure" of the active site (*5*). As the $P(r)$ differences are small, it is important to note that when the SAXS experiments were repeated using independent sample preparations, the same trends were observed.

Binding of phenylalanine to the free enzyme causes a conformational change. This change has been observed using a variety of techniques, including differential absorbance spectroscopy, fluorescence, protease sensitivity, sensitivity to sulfhydryl modifying reagents, analytical gel chromatography, and hydrodynamic measurements (*5*, *18*−*23*). To further analyze the role of these conformational changes in the allosteric mechanism, we compared the impact that alanine, 2-aminobutyric acid, and serine binding had on the SAXS signature of M_1-PYK (Figure 4). Binding of these three small amino acids elicits conformational changes very similar to those changes caused by phenylalanine binding.

As previously reported (*5*), PEP binding causes conformational changes in M_1-PYK (Figure 5). SAXS data were also measured for the ternary complexes containing one of the small amino acids and PEP. However, a study of the ternary complex that included phenylalanine and PEP was not possible because of the inability to simultaneously saturate the enzyme with both ligands (see Figure 2) within the solubility limit of phenylalanine. For alanine, 2-aminobutyric acid, and serine, conformational comparisons can be represented as (1) how the substrate (A) binds to the protein (E) in the absence or presence of the effector (X); [i.e., compare the $\Delta P(r)$ for E minus EA and the $\Delta P(r)$ for EX minus XEA] or (2) how the effector binds to the protein in the absence or presence of the substrate [i.e., compare the $\Delta P(r)$ for E minus EX and the $\Delta P(r)$ for EA minus XEA] (*3*). Following either comparative approach (Figure 5), it is clear that the ternary complexes of M_1-PYK with an amino acid and PEP are not

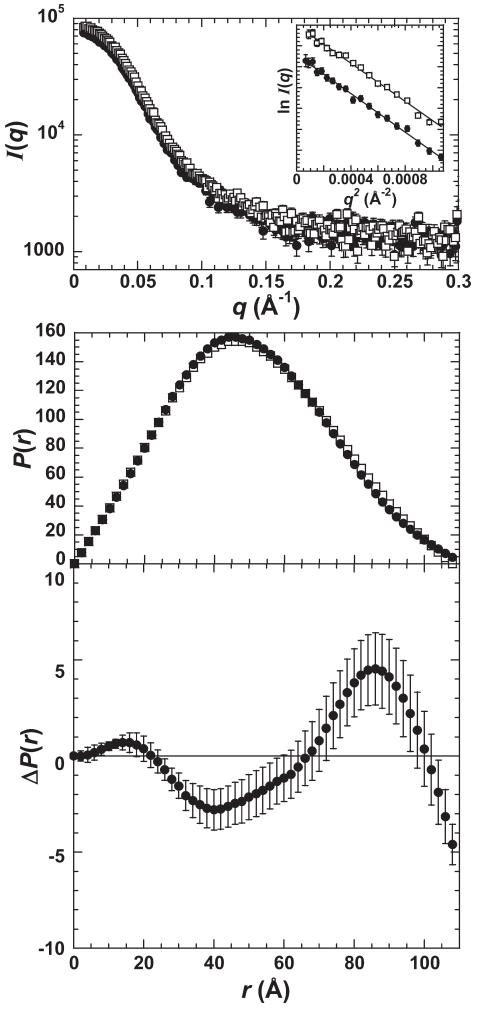

FIGURE 3: SAXS data for M_1-PYK. The top panel shows the $I(q)$ vs q function of free M_1-PYK (●) and the enzyme−Phe complex (□). The Guinier plot for the q range satisfying the $qR_g < 1.3$ condition is included in the inset (arbitrary y-axis units not included). The middle panel shows the $P(r)$ function derived from the SAXS profile of free M_1-PYK (●) and the enzyme−Phe complex (□). The bottom panel shows $\Delta P(r)$ between the free enzyme and the enzyme−Phe complex. Errors are based on propagated counting statistics; error bars are displayed for all data and when not apparent are smaller than the symbols.

Table 1: Structural Parameters Derived from the SAXS Data

	R_g (Å)	d_{max} (Å)	Porod volume ($\times 10^{-3}$ Å^3)
M_1-PYK	38.6 ± 0.1	108	189 ± 3
M_1-PYK−PEP	37.6 ± 0.3	110	188 ± 4
M_1-PYK−Phe	38.5 ± 0.2	112	192 ± 3
M_1-PYK−Ser	38.0 ± 0.2	108	194 ± 4
M_1-PYK−Ser−PEP	38.4 ± 0.2	108	191 ± 4
M_1-PYK−Ala	38.3 ± 0.2	110	184 ± 4
M_1-PYK−Ala−PEP	38.1 ± 0.2	110	179 ± 4
M_1-PYK−2AB	38.0 ± 0.3	112	185 ± 4
M_1-PYK−2AB−PEP	38.4 ± 0.27	110	180 ± 4

equivalent to protein complexes with only PEP bound or with only an amino acid bound. This finding suggests that each of these ligands (PEP and a small amino acid) influences how the other ligand binds to M_1-PYK.

The SAXS signatures in Figures 4 and 5 are similar, but not identical when the various amino acids are used. Therefore, consistent with the differences in fluorescence changes caused by the amino acids, small variations in conformation are likely. In

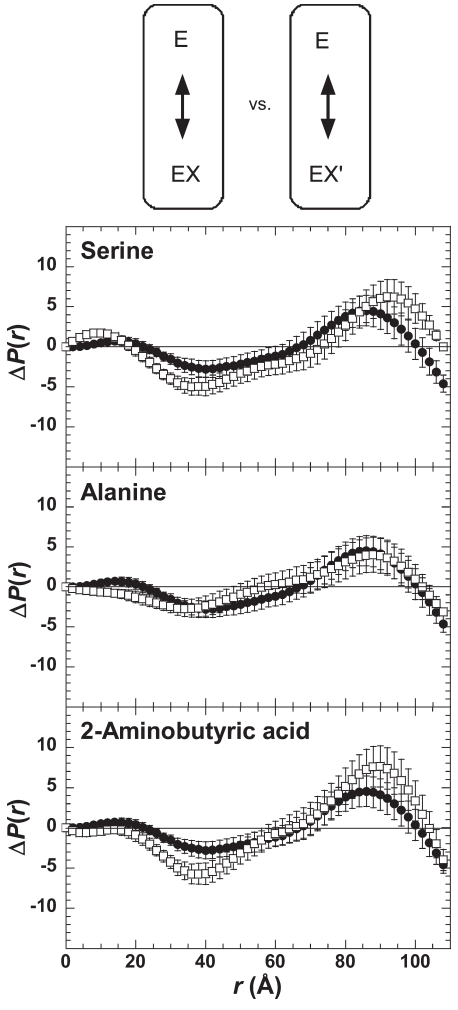

FIGURE 4: Comparisons of SAXS-characterized changes in the average conformation of M_1-PYK (E) elicited by binding of phenylalanine (X), vs alanine, 2-aminobutyric acid, or serine (X′). In each panel, the $\Delta P(r)$ between the free enzyme and the enzyme−Phe complex is shown as ● and the $\Delta P(r)$ that results from the binding of a second amino acid as □. Panels are labeled by the second amino acid included in the comparison. A schematic of the representative comparisons is shown above the panels; $\Delta P(r)$ data included in data panels are from comparisons within each circle in the schematic. In the schematic, E represents the enzyme, X phenylalanine, and X′ one of the small amino acids. Arrows within the schematic represent either the comparisons used to generate $\Delta P(r)$ data (within circles) or the comparisons made in each data panel (between circles). Errors are based on propagated counting statistics; error bars are displayed for all data and when not apparent are smaller than the symbols.

Figure 5, it is also noteworthy that the changes caused by amino acid binding appear to be similar to the changes caused by PEP binding. Interestingly, this may suggest that the EA and EX complexes are more similar to each other than either is to the free enzyme, a conclusion that is in contrast to that made in the previous study (*5*). We note that the previous neutron scattering study did not include the high salt concentrations that were required in our preparations to prevent protein aggregation, and that the neutron scattering experiments were performed in D_2O, which is known to alter the solubility properties of proteins.

DISCUSSION

Ligand binding often modifies protein conformation regardless of whether the protein demonstrates an allosteric regulation. In spite of this observation, when a protein is known to be

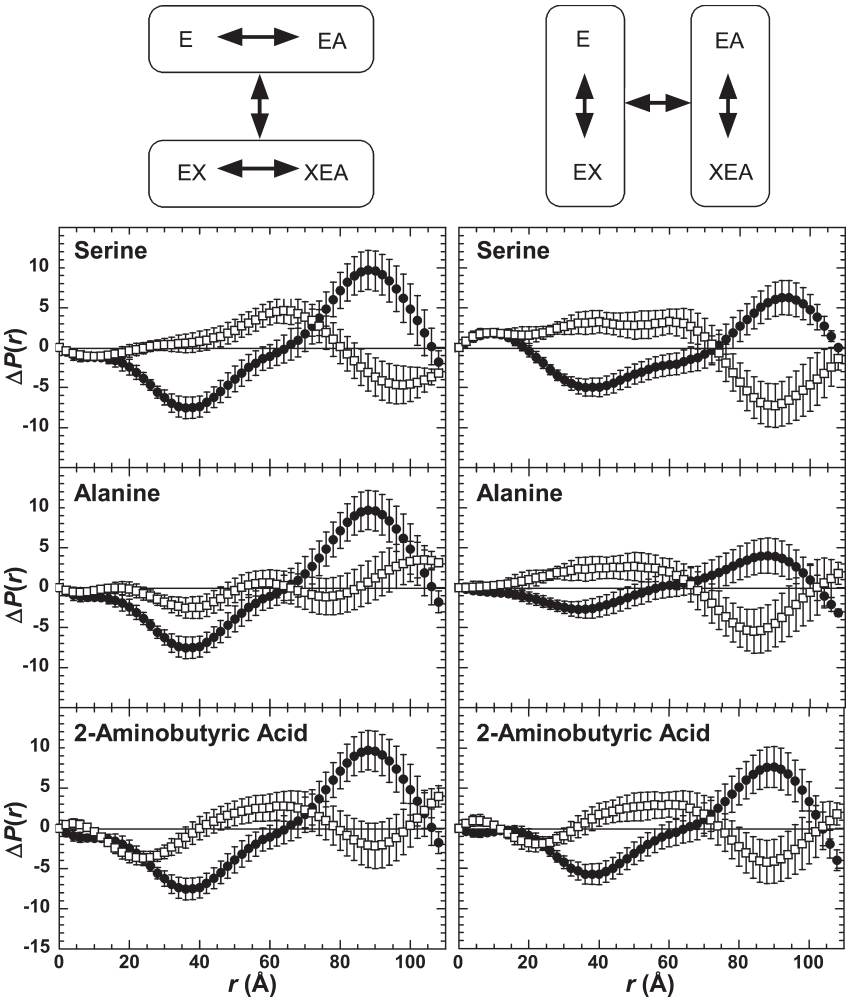

FIGURE 5: Comparisons of SAXS-characterized changes among the protein complexes in an allosteric energy cycle. As represented by the schematic above the panels, this energy cycle includes four enzyme complexes. Therefore, comparisons can be made in two ways. In panels and the schematic on the left, the $\Delta P(r)$ values associated with the binding of PEP are compared when an amino acid is absent (●) or present (□). In the panels and schematic on the right, the $\Delta P(r)$ values associated with the binding of an amino acid are compared when PEP is absent (●) or present (□). Data panels are labeled by the respective amino acid. Schematics of representative comparisons are shown above the panels; $\Delta P(r)$ data included in data panels are from comparisons within each circle within the schematic. In the schematic as in the data panels, E represents the enzyme and A represents PEP. In contrast to Figure 4, X represents any amino acid ligand. Arrows within the schematic represent either the comparisons used to generate $\Delta P(r)$ data (within circles) or the comparisons made in each data panel (between circles). Errors are based on propagated counting statistics; error bars are displayed for all data and when not apparent are smaller than the symbols.

allosterically regulated, there is a general trend to consider any and all conformational changes observed upon effector binding as having a role in the allosteric mechanism (*3*). Following this trend, the previous scattering studies of M_1-PYK were interpreted as if an all-or-none conformational change elicited by phenylalanine binding was the basis of the allosteric inhibition of PEP affinity (*5*, *24*). To further test this interpretation, we have monitored conformational changes with SAXS, both when phenylalanine binds and when the small amino acids bind. The data presented in Figure 4 demonstrate that the small amino acids are able to cause global conformational changes similar to those elicited by the allosteric effector, phenylalanine. Therefore, the global conformational changes of M_1-PYK observed upon amino acid ligand binding do not correlate with the ability of the amino acid to modify the affinity of the protein for PEP. Following the previous interpretation that scattering data monitor rotations of domains in M_1-PYK (*5*), domain rotations must be important for amino acid ligand binding. However, as the small amino acids that minimally modify PEP affinity elicit a SAXS-monitored conformational change similar to that caused by phenylalanine, clearly these rotations are not sufficient to describe the allosteric mechanism.

Rather than interpreting data in the context of an all-or-none change in global conformations, interpretations can focus on identifying response signatures (no matter how subtle) that are uniquely associated with individual amino acids. As one example, amino acid binding to the free enzyme elicits a range of fluorescence responses (Figure 1). In the structure of M_1-PYK, the nearest tryptophan residue is more than 20 Å from the amino acid binding site (*4*). Therefore, the variation in fluorescence intensity responses to the amino acids must reflect subtle conformational differences in the enzyme complexes when the various amino acids are bound. These subtle amino acid-dependent conformational differences may also be reflected in the observation that $\Delta P(r)$ functions, although very similar, are not completely identical (Figures 4 and 5). It then appears that each enzyme−ligand(s) complex may have distinct conformational features.

Distinct conformational features for each enzyme−ligand(s) complex are clearly inconsistent with the previously proposed two-state model (*24*). Unlike two-state mechanisms, a linked equilibrium

analysis (*3*, *10*−*13*) defines allostery as how the enzyme (E) binds its substrate (A) differently when the allosteric effector (X) is present versus absent. In the absence of the effector, substrate binding involves two enzyme complexes (E and EA). Likewise, when the effector is present, two protein complexes are involved in substrate binding (EX and XEA). Each of the four enzyme complexes (E, EA, EX, and XEA) can have unique conformational and/or dynamic properties. Because a linked equilibrium considers enzyme complexes rather than designated conformations, no restrictions and assumptions are made about conformational differences and similarities between, for example, M_1-PYK−phenylalanine and M_1-PYK−alanine complexes. Therefore, the data presented here are consistent with a linked equilibrium view of allostery.

On the basis of a linked equilibrium, allostery does not derive from a conformational transition resulting from the binding of a single ligand. Instead, how the binding of A (E compared to EA) changes when X is present (EX vs XEA) requires a comparison of four enzyme complexes, to identify allosterically relevant changes (*3*, *10*−*13*). Unfortunately, the inability to completely saturate the effector binding site with phenylalanine when PEP is present (Figure 2) prevents a full evaluation of the ternary complex of M_1-PYK with PEP and phenylalanine bound.

We were able to characterize the four relevant enzyme complexes when the effector ligand was one of the small amino acids (Figure 5). The impact of PEP binding on the SAXS signature is different when one of the small amino acids is present versus absent. These structural observations are consistent with each ligand (PEP and amino acid) mutually influencing how the other ligand binds to M_1-PYK. We found this result surprising given that the affinity of M_1-PYK for PEP is minimally altered by binding of the small amino acids. Taken together and using Ala as an example, it appears that PEP elicits different structural changes when binding to M_1-PYK versus M_1-PYK/Ala, although both enzyme species bind this substrate with similar affinity. This result might indicate some form of compensation within the allosteric mechanism. Both enthalpy and entropy compensation and compensation between multiple allosteric pathways have been identified in other allosteric proteins (*25*−*29*). However, confirming a compensatory mechanism was beyond the scope of the current work.

The goal of our study was to examine the relationship between allostery and the conformational changes that give rise to the signature changes in the $P(r)$ functions that were previously interpreted as representing a cleft closure. The question of whether it would be appropriate to use the now readily available three-dimensional modeling routines to attempt to generate a structural model of these changes and prove the earlier interpretation of domain rotation and cleft closure arises. We do not present such an analysis here as there are too many degrees of freedom in the tetrameric structure of M_1-PYK to prove a single three-dimensional model of domain rotation correct using the inherently one-dimensional scattering data; there are multiple ways that the observed mass redistribution could be accomplished. Importantly, we have used the simplest and most straightforward analysis that makes the fewest assumptions and does not suffer from the redundancy that is inherent in three-dimensional modeling of this multiple-subunit protein. Our difference $P(r)$ analysis definitively shows the lack of correlation between the SAXS signatures of conformational change and allostery. Nonetheless, we can consider the existing high-resolution crystal structure data and how it informs our thinking and supports

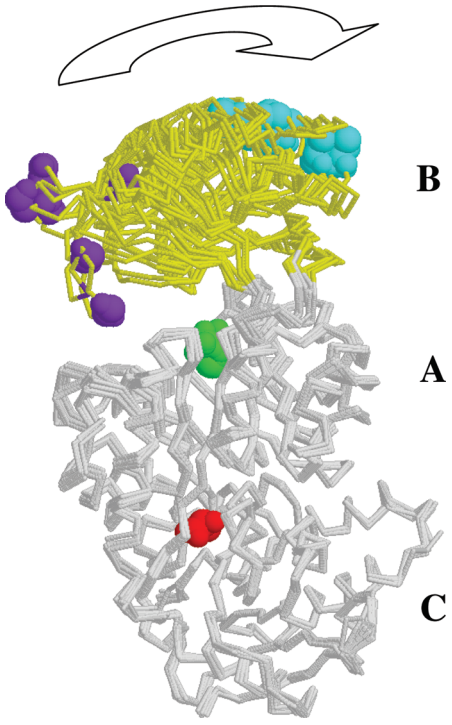

FIGURE 6: Overlay of M_1-PYK subunits as determined by X-ray crystallography. Of the 28 M_1-PYK subunits represented in various Protein Data Bank entries, subunits shown represent the 10 unique backbone traces (*4*, *31*−*35*). Each subunit has three domains (labeled A−C). The allosteric amino acid effector (red) binds between the A and C domains; this ligand is present in only one of the represented subunits. PEP [or a PEP analogue, pyruvate, oxalate, or phospholactate (green)] binds in the active site, between the A and B domains; most but not all subunits shown have a ligand present in the PEP binding site. Here, the B domain is colored yellow. To emphasize the motion of the B domain, two residues on the B domain are also colored (purple or cyan). However, this overlay does not provide evidence of global structural changes at the effector binding site; no additional global changes are observed upon comparison of tetramers (data not shown).

the domain rotation hypothesis. In the case of M_1-PYK, only a limited number of changes are revealed by comparison of X-ray crystallography-determined structures of M_1-PYK. The simplest summarization of these changes is that the B domain rotates with respect to other domains (Figure 6). Because of the location of the active site between the A and B domains, it seems reasonable to speculate that PEP binding to the active site influences B domain rotation and is influenced by B domain rotation. However, the same structural comparisons do not give insight into a potential signaling mechanisms by which ligand binding to the allosteric amino acid binding site influences the active site (PEP binding or B domain rotation) (Figure 6). Instead, previous speculation regarding signaling mechanisms is derived from comparisons of structures from many different isozymes (*6*−*8*); given that single mutations alter allosteric regulation (*30*), proposed allosteric mechanisms derived from structural comparisons among isozymes should be viewed with caution. Of particular interest, the structure with alanine bound (*4*) does not reveal changes in the vicinity of the effector binding site or global conformational changes that have not already been identified by comparisons among structures with no effector present (Figure 6). One potential reason might be constraints due to crystal lattice formation. However, it is also possible that the conditions used for crystal growth result in a structure that is not "allosterically competent",

used here in the same way crystallographic data for enzymes are often discussed as being in enzymatically competent forms. It is important to note that solution studies of M_1-PYK most generally include Mg^{2+} to satisfy the divalent cation requirement for catalysis. However, with only a few exceptions, structures of M_1-PYK have been determined with Mn^{2+} present in the active site (*4*, *31*−*35*). The allosteric functions of both yeast and human liver pyruvate kinase isozymes are dependent on the type of divalent cation present in the active site (*36*−*40*). If the same trend is true in M_1-PYK, then this effect would have to be taken into account in comparing high-resolution structures and solution studies.

In summary, amino acid binding elicits conformational changes in M_1-PYK, regardless of whether this binding event alters $K_{app\text{-}PEP}$. All amino acids tested elicit similar but not identical conformational changes. Both the similar global responses to the amino acids that do and do not modify $K_{app\text{-}PEP}$ and the subtle variations among the complexes investigated are inconsistent with the previously proposed two-state mechanism (*24*). However, these results can be accommodated by a linked equilibrium view of allostery that allows each enzyme complex to have unique conformational properties (*3*). This view of allostery also allows a compensating mechanism to contribute to the observed free energy associated with allostery. The finding that the small amino acids influence the conformational changes that PEP causes when it binds to M_1-PYK allows us to speculate that the small amino acids do not modify $K_{app\text{-}PEP}$ because of a compensating mechanism.

ACKNOWLEDGMENT

We thank Drs. Antonio Artigues and Cy Jeffries for critically reading an early version of the manuscript and making very helpful suggestions. Initial subunit overlays were generated as a project directed by Randy Dix in the Biotechnology/Life Sciences Program at Olathe North High School, Olathe, KS; we appreciate contributions from Mr. Dix and his high school students.

REFERENCES

1. Carminatti, H., Jimenez de Asua, L., Leiderman, B., and Rozengurt, E. (1971) Allosteric properties of skeletal muscle pyruvate kinase. *J. Biol. Chem. 246*, 7284–7288.
2. Kayne, F. J., and Price, N. C. (1973) Amino acid effector binding to rabbit muscle pyruvate kinase. *Arch. Biochem. Biophys. 159*, 292–296.
3. Fenton, A. W. (2008) Allostery: An illustrated definition for the 'second secret of life'. *Trends Biochem. Sci. 33*, 420–425.
4. Williams, R., Holyoak, T., McDonald, G., Gui, C., and Fenton, A. W. (2006) Differentiating a Ligand's Chemical Requirements for Allosteric Interactions from Those for Protein Binding. Phenylalanine Inhibition of Pyruvate Kinase. *Biochemistry 45*, 5421–5429.
5. Consler, T. G., Uberbacher, E. C., Bunick, G. J., Liebman, M. N., and Lee, J. C. (1988) Domain interaction in rabbit muscle pyruvate kinase. II. Small angle neutron scattering and computer simulation. *J. Biol. Chem. 263*, 2794–2801.
6. Valentini, G., Chiarelli, L. R., Fortin, R., Dolzan, M., Galizzi, A., Abraham, D. J., Wang, C., Bianchi, P., Zanella, A., and Mattevi, A. (2002) Structure and function of human erythrocyte pyruvate kinase. Molecular basis of nonspherocytic hemolytic anemia. *J. Biol. Chem. 277*, 23807–23814.
7. Jurica, M. S., Mesecar, A., Heath, P. J., Shi, W., Nowak, T., and Stoddard, B. L. (1998) The allosteric regulation of pyruvate kinase by fructose-1,6-bisphosphate. *Structure 6*, 195–210.
8. Rigden, D. J., Phillips, S. E., Michels, P. A., and Fothergill-Gilmore, L. A. (1999) The structure of pyruvate kinase from *Leishmania mexicana* reveals details of the allosteric transition and unusual effector specificity. *J. Mol. Biol. 291*, 615–635.
9. Oberfelder, R. W., and Lee, J. C. (1985) Measurement of ligand-protein interaction by electrophoretic and spectroscopic techniques. *Methods Enzymol. 117*, 381–399.
10. Weber, G. (1972) Ligand binding and internal equilibria in proteins. *Biochemistry 11*, 864–878.
11. Reinhart, G. D. (2004) Quantitative analysis and interpretation of allosteric behavior. *Methods Enzymol. 380*, 187–203.
12. Reinhart, G. D. (1983) The determination of thermodynamic allosteric parameters of an enzyme undergoing steady-state turnover. *Arch. Biochem. Biophys. 224*, 389–401.
13. Reinhart, G. D. (1988) Linked-function origins of cooperativity in a symmetrical dimer. *Biophys. Chem. 30*, 159–172.
14. Boyer, P. D. (1962) Pyruvate Kinase. In The Enzymes (Boyer, P. D., Lardy, H. A., and Myrback, K., Eds.) 2nd ed., pp 95−113, Academic Press, New York.
15. Heidorn, D. B., and Trewhella, J. (1988) Comparison of the crystal and solution structures of calmodulin and troponin C. *Biochemistry 27*, 909–915.
16. Svergun, D. I. (1991) Mathematical methods in small-angle scattering data analysis. *J. Appl. Crystallogr. 24*, 485–492.
17. Porod, G. (1951) Die Roentgenkleinwinkel-Steuung von Dichtgepackten Kolloiden Systemen, I Teil. *Kolloid Z. Z. Polym. 124*, 83–111.
18. Oberfelder, R. W., Barisas, B. G., and Lee, J. C. (1984) Thermodynamic linkages in rabbit muscle pyruvate kinase: Analysis of experimental data by a two-state model. *Biochemistry 23*, 3822–3826.
19. Heyduk, E., Heyduk, T., and Lee, J. C. (1992) Global conformational changes in allosteric proteins. A study of *Escherichia coli* cAMP receptor protein and muscle pyruvate kinase. *J. Biol. Chem. 267*, 3200–3204.
20. Consler, T. G., and Lee, J. C. (1988) Domain interaction in rabbit muscle pyruvate kinase. I. Effects of ligands on protein denaturation induced by guanidine hydrochloride. *J. Biol. Chem. 263*, 2787–2793.
21. Kayne, F. J., and Price, N. C. (1972) Conformational changes in the allosteric inhibition of muscle pyruvate kinase by phenylalanine. *Biochemistry 11*, 4415–4420.
22. Kwan, C. Y., and Davis, R. C. (1981) L-Phenylalanine induced changes of sulfhydryl reactivity in rabbit muscle pyruvate kinase. *Can. J. Biochem. 59*, 92–99.
23. Kwan, C. Y., and Davis, R. C. (1980) pH-dependent amino acid induced conformational changes of rabbit muscle pyruvate kinase. *Can. J. Biochem. 58*, 188–193.
24. Lee, J. C. (2008) Modulation of allostery of pyruvate kinase by shifting of an ensemble of microstates. *Acta Biochim. Biophys. 40*, 663–669.
25. Fisher, H. F., and Tally, J. (1998) Isoergonic cooperativity: A novel form of allostery. *Methods Enzymol. 295*, 331–349.
26. Fisher, H. F., and Tally, J. (1997) Isoergonic cooperativity in glutamate dehydrogenase complexes: A new form of allostery. *Biochemistry 36*, 10807–10810.
27. Tlapak-Simmons, V. L., and Reinhart, G. D. (1998) Obfuscation of allosteric structure-function relationships by enthalpy-entropy compensation. *Biophys. J. 75*, 1010–1015.
28. Braxton, B. L., Tlapak-Simmons, V. L., and Reinhart, G. D. (1994) Temperature-induced inversion of allosteric phenomena. *J. Biol. Chem. 269*, 47–50.
29. Fenton, A. W., and Reinhart, G. D. (2009) Disentangling the Web of Allosteric Communication in a Homotetramer: Heterotropic Inhibition in Phosphofructokinase from *Escherichia coli*. *Biochemistry 48*, 12323–12328.
30. Ikeda, Y., Tanaka, T., and Noguchi, T. (1997) Conversion of non-allosteric pyruvate kinase isozyme into an allosteric enzyme by a single amino acid substitution. *J. Biol. Chem. 272*, 20495–20501.
31. Larsen, T. M., Benning, M. M., Rayment, I., and Reed, G. H. (1998) Structure of the bis(Mg^{2+})-ATP-oxalate complex of the rabbit muscle pyruvate kinase at 2.1 Å resolution: ATP binding over a barrel. *Biochemistry 37*, 6247–6255.
32. Larsen, T. M., Benning, M. M., Wesenberg, G. E., Rayment, I., and Reed, G. H. (1997) Ligand-induced domain movement in pyruvate kinase: Structure of the enzyme from rabbit muscle with Mg^{2+}, K^+, and L-phospholactate at 2.7 Å resolution. *Arch. Biochem. Biophys. 345*, 199–206.
33. Larsen, T. M., Laughlin, L. T., Holden, H. M., Rayment, I., and Reed, G. H. (1994) Structure of rabbit muscle pyruvate kinase complexed with Mn^{2+}, K^+, and pyruvate. *Biochemistry 33*, 6301–6309.
34. Wooll, J. O., Friesen, R. H., White, M. A., Watowich, S. J., Fox, R. O., Lee, J. C., and Czerwinski, E. W. (2001) Structural and functional linkages between subunit interfaces in mammalian pyruvate kinase. *J. Mol. Biol. 312*, 525–540.
35. Stuart, D. I., Levine, M., Muirhead, H., and Stammers, D. K. (1979) Crystal structure of cat muscle pyruvate kinase at a resolution of 2.6 Å. *J. Mol. Biol. 134*, 109–142.
36. Fenton, A. W. (2009) Chapter 5: The Impact of Ions on Allosteric Functions in Human Liver Pyruvate Kinase. *Methods Enzymol. 466*, 83–107.

37. Bollenbach, T. J., and Nowak, T. (2001) Kinetic linked-function analysis of the multiligand interactions on Mg^{2+}-activated yeast pyruvate kinase. *Biochemistry 40*, 13097–13106.
38. Bollenbach, T. J., and Nowak, T. (2001) Thermodynamic linked-function analysis of Mg^{2+}-activated yeast pyruvate kinase. *Biochemistry 40*, 13088–13096.
39. Mesecar, A. D., and Nowak, T. (1997) Metal-ion-mediated allosteric triggering of yeast pyruvate kinase. 2. A multidimensional thermodynamic linked-function analysis. *Biochemistry 36*, 6803–6813.
40. Mesecar, A. D., and Nowak, T. (1997) Metal-ion-mediated allosteric triggering of yeast pyruvate kinase. 1. A multidimensional kinetic linked-function analysis. *Biochemistry 36*, 6792–6802.